ELSEVIER

Journal of Nuclear Materials 251 (1997) 132–138

journal of nuclear materials

Studies of defects and defect agglomerates by positron annihilation spectroscopy

M. Eldrup *, B.N. Singh

Materials Research Department, Risø National Laboratory, DK-4000 Roskilde, Denmark

Abstract

A brief introduction to positron annihilation spectroscopy (PAS), and in particular to its use for defect studies in metals is given. Positrons injected into a metal may become trapped in defects such as vacancies, vacancy clusters, voids, bubbles and dislocations and subsequently annihilate from the trapped state in the defect. The annihilation characteristics (e.g., the lifetime of the positron) can be measured and provide information about the nature of the defect (e.g., size, density, morphology). The technique is sensitive to both defect size (in the range from monovacancies up to cavities containing 50–100 vacancies) and density in metals. Monovacancies can typically be detected in concentrations higher than a tenth of a part per million. For three dimensional vacancy clusters the sensitivity increases with increasing cluster size. The combination of PAS with theoretical calculations and with other experimental methods (in particular transmission electron microscopy) forms the basis for the use of PAS to quantitatively characterize defects and defect complexes, both visible and invisible in transmission electron microscopes; this is illustrated by some examples. Finally, the advantages of the use of PAS are pointed out. © 1997 Elsevier Science B.V.

PACS: 78.70.Bj; 71.60.+z; 61.70.−r; 61.80.−x

1. Introduction

The use of positron annihilation spectroscopy (PAS) for studies of defects in solids is mainly based on two facts. The first one is that positrons are antiparticles to electrons so that a positron may annihilate with an electron. An amount of energy, equivalent to the mass of the two particles, will then be emitted simultaneously with the annihilation, normally as gamma radiation that carry information about the state of the positron–electron pair before annihilation. The second fact is that positrons injected into a material may get trapped in defects and annihilate there (rather than in the bulk material). By suitable measurements of the emitted gamma quanta it is then possible to obtain useful information about the characteristics of those defects that trap the positrons. In this note we shall briefly describe some of the physical basis of PAS and how it can be used in defect studies; some examples will be provided, mainly from work in our own laboratory. More detailed discussions of PAS can be found, for example, in Refs. [1–5].

2. Positrons in solids

In conventional positron annihilation experiments, the positrons are injected into a sample from a radioactive source (e.g., ^{22}Na) which emits positrons with a mean energy of a few hundred keV. The injected positrons slow down to thermal energies in about 10^{-12}–10^{-11} s by ionization and excitation of the atoms of the solid. During thermalization, the positrons penetrate the solid to an average depth of about 20 mg/cm^2 (i.e., in metals roughly 20–100 μm). Hence, the positrons probe bulk material in such measurements. In recent years the development of beams of monoenergetic positrons whose energy can be

* Corresponding author. Tel.: +45-46 77 5728; fax: +45-46 77 5758; e-mail: morten.eldrup@risoe.dk.

PII S0022-3115(97)00221-3

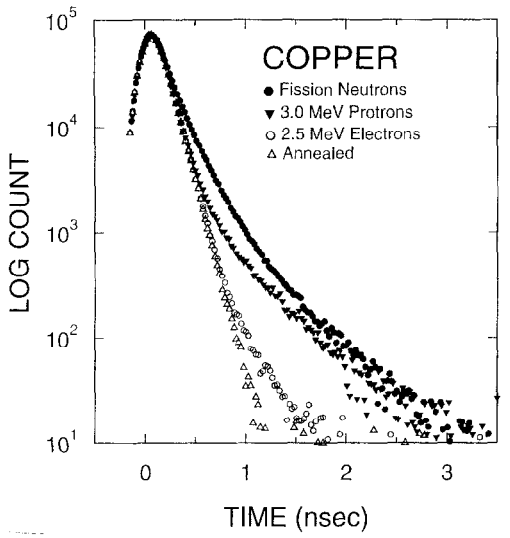

Fig. 1. Positron lifetime spectra for annealed copper, and for copper irradiated with electrons, protons and neutrons to a dose level of ~0.01 dpa. Irradiations were carried out at ~523 K. The long-lived components of the spectra (> ~1 ns) for the irradiated samples are due to the presence of defects, mainly voids [10].

varied over a wide range has taken place. With such beams, also thin surface layers may be investigated [3,6–8].

After a positron has been injected into a solid and has thermalized, it will in most cases annihilate with the emission of two γ-quanta, each of them with an energy of 511 keV (the equivalent to the electron rest mass). The two γ-rays will be emitted in almost opposite directions. Small deviations from an angle of exactly 180° are due to deviations from zero of the total electron–positron momentum (because of momentum conservation in the annihilation process). By measuring these deviations from 180°, the distribution of the total momentum of the annihilating particles may be determined. In metals in particular, the positron momentum is low compared to that of the electrons and the measurements therefore determine the electron momentum, i.e., the electronic structure [1–5,9].

The rate at which the positrons annihilate with the electrons in the medium is proportional to the density of electrons at the site of the positron. Therefore the mean lifetime of positrons ($\tau = \lambda^{-1}$, where λ is the annihilation rate) is a measure of the electron density at the positions of the positrons [1–5], in such a way that a lower electron density is reflected in a longer positron lifetime.

In this short contribution we shall not describe the experimental techniques, but refer to, for example, Refs. [1–5]. It should be pointed out, however, that techniques are available for the measurements of both momentum distributions (angular correlation and Doppler broadening techniques) and positron lifetime distributions. An example of the latter is shown in Fig. 1. It shows so-called positron lifetime spectra for annealed copper as well as for copper irradiated with electrons, protons or neutrons [10]. The spectra consist of sums of decaying exponentials (that are somewhat smeared because of the finite time resolution of the lifetime spectrometer). The spectrum for annealed Cu contains one, short-lived component, while the spectra for the irradiated copper include also long-lived components that arise from positrons trapped mainly in voids.

3. Positron trapping and annihilation in defects

In the following we shall briefly describe the behavior of positrons in metals with special reference to trapping in defects. In semiconductors and insulators, for example, the picture is similar, but somewhat more complicated [11,12].

In a perfect metal lattice, the injected positrons will, after thermalization, diffuse ~100–200 nm during their lifetime. This lifetime of 100–400 ps depends upon the metal [11]. If the metal contains defects such as vacancies, vacancy clusters (including voids and bubbles) and dislocations, i.e., regions of less than average atomic density, positrons may become trapped, i.e., localized at these defects. This is because the positron is repelled by the positively charged ion cores. Hence, structural defects with missing, or a reduced density of, ions will provide attractive potentials for positrons (more details in Ref. [11]). Trapped in such a defect, the positron will experience a lower electron density than in the bulk material and its lifetime will therefore increase. Furthermore, the average momentum of the electrons at the defect is lower than in the bulk which results in a narrower total-momentum distribution for the annihilation quanta. These measurable changes in annihilation characteristics for defect-trapped positrons are the basis for the now well established use of PAS for metal defect studies.

The annihilation characteristics depend on the type of defect in which the positron is trapped. Hence it is possible in many cases to differentiate between different types of defects. From the rates at which the defects trap positrons, defect concentrations can be derived. For example, for positrons trapped in three dimensional vacancy clusters their lifetime will generally increase with cluster size as illustrated by the calculated curves shown in Fig. 2 [13]. This is so because with increasing cavity size the average electron density inside the cavity, where the positron is localized, will decrease. For large cavities though, the positron will be localized at the cavity surface, and the lifetime (~500 ps) will no longer depend on the size. If however, the vacancy cluster contains helium, the electrons of the He will overlap with the trapped positron and the lifetime of the positron will therefore be reduced. Fig. 2 shows the influence of the presence of helium on the lifetime of the trapped positron.

For larger, three dimensional vacancy clusters (voids) the positron lifetime approaches ~500 ps as mentioned

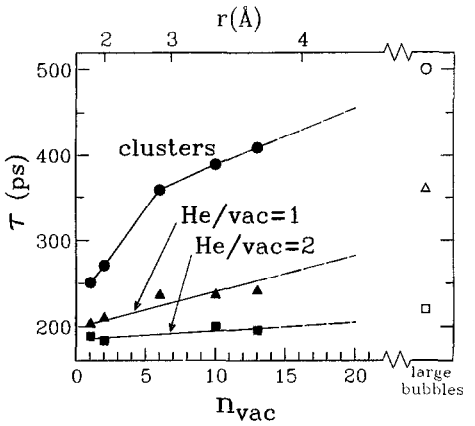

Fig. 2. The positron lifetime calculated for a positron trapped in a small three dimensional vacancy cluster in aluminum as a function of the number of vacancies in the cluster (n_{vac}) and for different helium to vacancy ratios in the clusters (i.e. no He, 1 He and 2 He atoms for each vacancy). The upper scale shows the cluster radius. In a perfect Al lattice the lifetime is 165 ps. From Ref. [13].

above. However, like for small clusters (Fig. 2), if the void contains gas atoms, the positron lifetime will be reduced. This reduction will increase with increasing gas density as illustrated by the calculated results for He bubbles in Al, shown in Fig. 3 [13]. Thus, for small cavities, the positron lifetime is influenced by both the cavity size and the gas density in the cavities, while for large voids ($> \sim 50$–100 vacancies) the lifetime is not sensitive to size, but only to gas density. In general, theoretical calculations of positron lifetimes have been found to be in good agreement with experimental results [11,14].

The trapping of positrons into defects takes place in competition with the annihilation of the positrons in the bulk. If only one type of traps is present, the following two simple rate equations have been used to derive the probabilities that the positron is in the bulk (P_b) and in the defect (P_d) [1–5]:

$$\frac{dP_b}{dt} = -\lambda_b P_b - \kappa P_b, \tag{1}$$

$$\frac{dP_d}{dt} = -\lambda_d P_d + \kappa P_b, \tag{2}$$

where κ is the trapping rate and λ_b and λ_d are the annihilation rates in the bulk and in the defect, respectively. The solutions to these equations lead to a lifetime spectrum with two exponential components with the lifetimes:

$$\tau_1 = (\lambda_b + \kappa)^{-1}, \qquad \tau_2 = \lambda_d^{-1} \tag{3}$$

and relative intensities:

$$I_1 = 1 - I_2, \qquad I_2 = \kappa(\lambda_b - \lambda_d + \kappa)^{-1}. \tag{4}$$

These equations can easily be expanded to include more than one type of defects with different annihilation rates λ_{di} and trapping rates κ_i. Normally, it is a good approximation to assume that the trapping rate into one type of defects is proportional to the density, C_i, of that defect type, i.e.,

$$\kappa_i = \mu_i C_i. \tag{5}$$

The so-called specific trapping rate, μ_i, depends on the

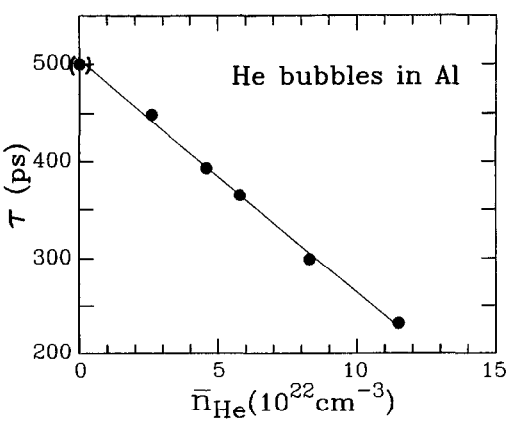

Fig. 3. The lifetime calculated for a positron trapped in a He bubble ($n_{vac} > \sim 50$) in aluminum as a function of helium density (n_{He}) in the bubble (filled circles). The straight line through the points gives the relationship $\tau = 500 - 23.5 n_{He}$, with τ in ps and n_{He} in 10^{28} m^{-3}. From Ref. [13].

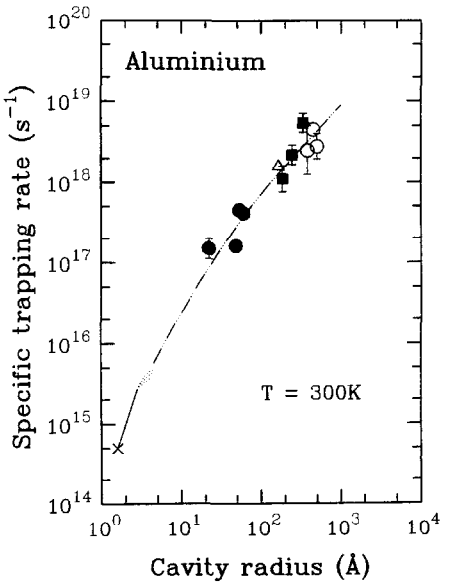

Fig. 4. Estimate of the specific trapping rate, μ, for positrons into spherical cavities as a function of cavity size in Al (filled symbols for He bubbles, open symbols for voids). The chain curve is a fit of a theoretical model to the points. The cross is for a monovacancy. The cavity radii are mean values obtained by TEM. From Ref. [15].

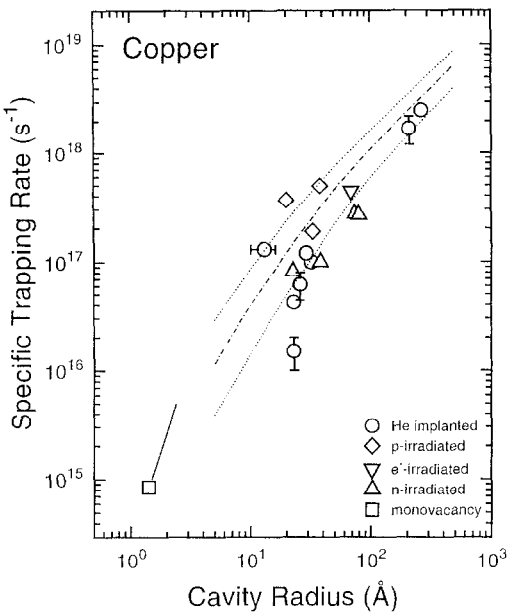

Fig. 5. Estimate of the specific trapping rate, μ, for positrons into spherical cavities as a function of cavity size in Cu. The chain curve is an estimate based on the curve for Al, and the dotted curves represent expected uncertainty bands. The cavity radii are mean values obtained by TEM. From Ref. [16].

type of defects. The specific trapping rate for monovacancies in aluminum, for example, is about 5×10^{14} s^{-1}. If the vacancy density is 0.1 at.ppm, κ_i will then be 5×10^7 s^{-1} (Eq. (5)) which leads to an intensity of the defect component of $I_2 = 2.5\%$ (Eq. (4)). This intensity value is roughly the practical experimental detection limit. Thus, the sensitivity of PAS to vacancies is roughly a tenth of a part per million. For spherical cavities μ_i increases strongly with cavity size as shown for aluminum in Fig. 4 [15] and for copper in Fig. 5 [16].

4. Application to defect studies

The lifetimes and intensities of the various spectral components in a measured lifetime spectrum can be extracted by fitting a sum of decaying exponentials to the spectrum. Using the quantitative relationships between the extracted lifetime parameters and defect characteristics like the ones discussed above, it is possible to extract quantitative information about the defect population. In the following, we shall illustrate this by briefly discussing some experimental results obtained in our laboratory on vacancies, voids and helium bubbles. These results are on (1) void formation by annealing of electron irradiated molybdenum, (2) void formation in neutron, proton and electron irradiated copper, (3) coarsening of helium bubbles in aluminum on annealing and (4) the annealing behavior of small vacancy clusters and helium bubbles in He implanted copper.

4.1. Electron irradiated molybdenum

An early experiment which took advantage of the sensitivity of PAS to monovacancies is described in Ref. [18]. Frenkel pairs were created at room temperature in molybdenum by 10 MeV electron irradiation. The presence of monovacancies in the as-irradiated Mo was detected by both positron lifetime and angular correlation measurements. The lifetime measurements, for example, showed the presence of a component due to vacancies with $\tau_2 \sim$ 200 ps, considerably longer than the 120 ps observed for well annealed Mo. On annealing above $\sim$ 450 K (stage III) a strong increase of τ_2 up to $\sim$ 450 ps and a simultaneous decrease in the intensity, I_2, of this component was observed. The increase of τ_2 showed that three dimensional vacancy clusters were formed in stage III, i.e., that vacancies were migrating in this annealing stage. The decrease of the intensity reflects that some vacancies were lost to sinks or recombined with self interstitials during migration. In addition, the positron trapping rate per vacancy decreases with increasing cluster size. This also contributed to the reduction of I_2 (Eqs. (4) and (5)). No cavities could be observed by TEM in the as-irradiated specimens or after annealing up to $\sim$ 700 K. However, after annealing to $\sim$ 1175 K, the presence of voids, grown during the annealing, was confirmed by TEM.

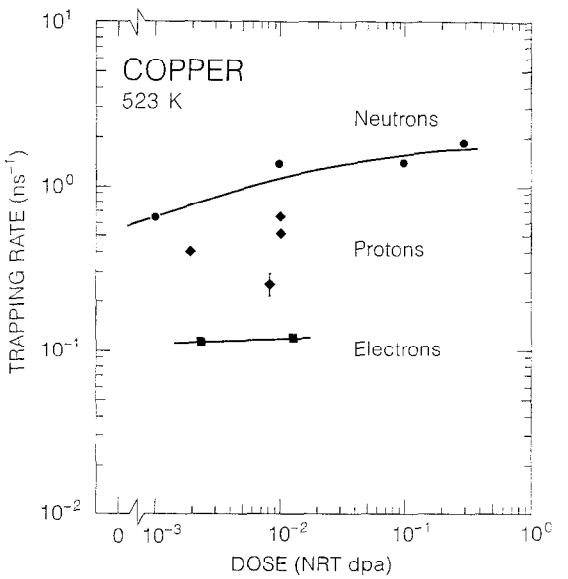

Fig. 6. The dose dependence of the positron trapping rates into voids in copper, created by irradiation at 523 K with fission neutrons, 3 MeV protons, or 2.5 MeV electrons. The mean void diameters determined by TEM are 76 Å, 71 Å and 138 Å, respectively for a dose of about 0.01 dpa. From Ref. [10].

4.2. Voids in neutron, proton and electron irradiated copper

The lifetime spectra in Fig. 1 show a higher intensity of the long-lived portion of the spectrum for neutron irradiated copper than for proton and electron irradiated specimens. In order to quantify this effect, these spectra as well as spectra for other irradiation doses were analyzed and the trapping rates into voids were calculated by use of formulae equivalent to those given above. The deduced trapping rates are shown in Fig. 6. The rates depend weakly on the radiation dose, but in particular on the type of particle used for the irradiation. Since the void diameters show only a minor variation (7.1–13.8 nm), the main reason for the variation in trapping rate is the variation in void density. This is in agreement with the observations by TEM that shows that the void density varies in a wide range from about 5×10^{18} m^{-3} (electron irradiated) to about 6×10^{20} m^{-3} (neutron irradiation). This confirmation of the TEM results by PAS is particularly important for the case of low void densities in the electron irradiated sample, where large statistical fluctuations may occur in the TEM observations. Furthermore, the PAS results show that no population of invisible cavities is present in these samples. The

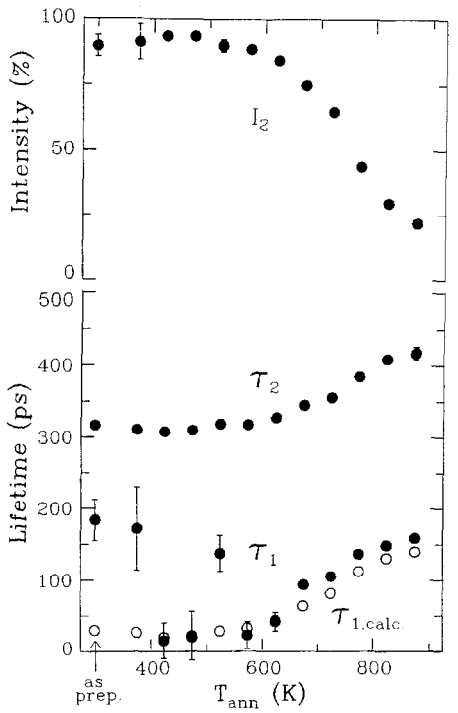

Fig. 7. The annealing behavior of the positron lifetime parameters for aluminum that contains helium bubbles (generated by irradiation at ~ 380 K with 600 MeV protons to a dose of 0.35 dpa which results in a He content of ~ 75 at.ppm.) τ_2 is the lifetime associated with positrons trapped in the He bubbles, and I_2 its intensity. From Refs. [15,19].

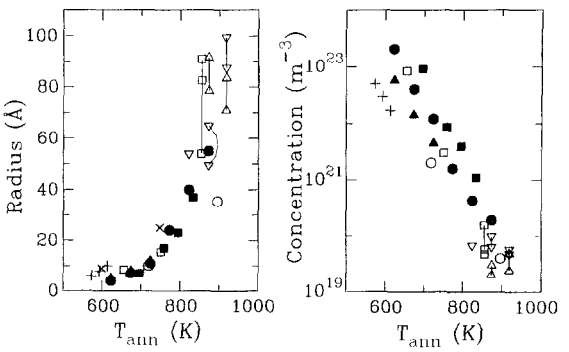

Fig. 8. The radius and density of helium bubbles in aluminum as functions of the annealing temperature. The filled circles, triangles and squares are derived from the results of the positron lifetime measurements shown in Fig. 7 and other similar measurements, the other symbols represent literature TEM data for similarly treated specimens. From Ref. [19].

increase in the cavity density with increasing damage energy has been interpreted to be due to an increase in the vacancy supersaturation [16] resulting from the enhanced clustering of the self-interstitial atoms in cascades produced under proton and neutron irradiations. This is consistent with the predictions of the production bias model [17].

4.3. Helium bubbles in aluminum

Fig. 7 shows the annealing behavior of positron lifetime parameters for helium bubbles in aluminum generated by 600 MeV proton irradiation at about 380 K [15,19]. In spite of a He content of about 75 at.ppm produced in the sample by transmutation, no He bubbles could be observed in the bulk material by TEM after irradiation at this temperature. However, in the as-irradiated material PAS shows the presence of an intense long lifetime component with $\tau_2 = 320$ ps which is the clear signature of a high density of small cavities, mostly bubbles [19]. On annealing above ~ 600 K, τ_2 increases. In part this may be due to an increase in bubble size, but in particular a decrease in the He density in the bubbles (see Figs. 2 and 3). The strong decrease of the intensity I_2 shows that the density of bubbles decreases. Using the quantitative relationships shown above (Eqs. (4) and (5), the specific trapping rate, μ, versus radius in Fig. 4 and the lifetime, τ, versus helium density, n_{He}, in Fig. 3), estimates of bubble sizes and densities could be obtained that were in good agreement with data from TEM on similar specimens, as shown in Fig. 8 [19].

4.4. Helium implanted copper

Fig. 9 shows the lifetime and intensity of the longlived component for the annealing of copper that had been implanted with He at two different temperatures [16]. For

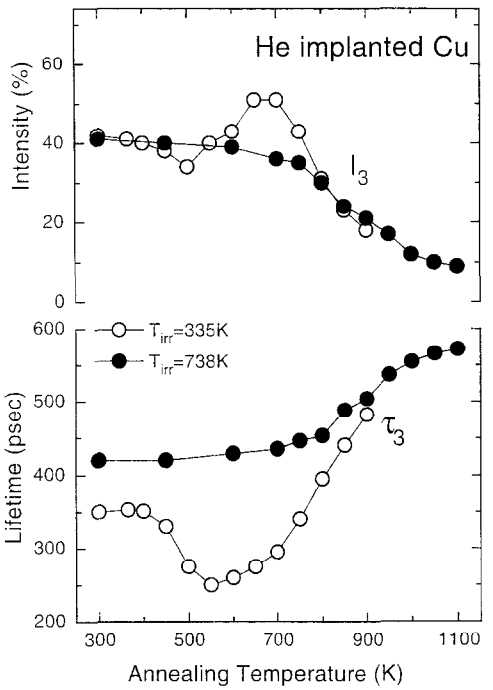

Fig. 9. The annealing behavior of positron lifetime parameters for copper that had been implanted at two different temperatures with He to the doses 110 at.ppm (○) and 340 at.ppm (●). The lifetime τ_3 and its intensity I_3 are associated with positrons trapped in He bubbles and/or small vacancy clusters as discussed in the text. From Ref. [16].

Cu implanted at 738 K (filled circles), He bubbles with a mean diameter of 5.8 nm were observed by TEM in the as-implanted specimens [20]. On annealing above the implantation temperature, coarsening of the bubbles is seen by the increase of the lifetime and simultaneous decrease of its intensity. After implantation at 335 K (open circles), no cavities could be observed by TEM in the as-implanted specimens. However, the positron lifetime of about 350 ps is clear evidence of the presence of small cavities, with or without He atoms. On annealing, the lifetime decreases to a minimum at about 550 K and then increases. This decrease may be ascribed to a decrease in size of the clusters due to thermal emission of vacancies and/or an influx of He atoms from the dissociation of other small clusters. At higher temperatures coarsening into bubbles takes place as evidenced by the increase of the lifetime and decrease of its intensity. This example once more illustrates how PAS can supplement TEM by giving information about submicroscopic defect clusters.

5. Conclusions

The examples described in the present note serve to illustrate two major advantages of PAS. One is that positrons are sensitive to defects in the size range from monovacancies up to cavities that can be seen by TEM and in the density range (for monovacancies) above roughly a tenth of a part per million. For clusters of vacancies, the sensitivity is higher. In addition, PAS can give information about rare gas densities in bubbles. The sampling volume for conventional positron annihilation spectroscopy is typically about 0.1 mm^3 and the defect characteristics that can be derived from the measurements are therefore volume averaged. This makes the technique a useful supplement to TEM investigations, in particular for low defect densities where TEM results may be subject to significant fluctuations. With variable-energy positron beams, on the other hand, depth profiling of defect densities close to surfaces is possible. Finally it should be mentioned that the technique is non-destructive. This means that for a full annealing study, for example, only one set of specimens is necessary.

Acknowledgements

This work was partly funded by the European Fusion Technology Programme.

References

[1] P. Hautojärvi, ed., Positrons in Solids (Springer, Berlin, 1979).
[2] W. Brandt, A. Dupasquier, eds., Positron Solid-State Physics (North Holland, Amsterdam, 1983).
[3] A. Dupasquier, A.P. Mills, eds., Positron Spectroscopy of Solids (North-Holland, Amsterdam, 1994).
[4] M. Eldrup, in: Defects in Solids, eds. A.V. Chadwick and M. Terenzi (Plenum, New York, 1986) p. 145.
[5] M. Eldrup, J. Phys. (Paris) IV Colloq. 5 (1995) C1–93.
[6] P.J. Schultz, K.G. Lynn, Rev. Mod. Phys. 60 (1988) 701.
[7] M. Doyama, T. Akahane, M. Fujinami, eds., SLOPOS-6, Appl. Surf. Sci. 85 (1995) pp. 1–344.
[8] D.W. Lawther, P.J. Simpson, Defect Diffus. Forum 138&139 (1996) 1.
[9] R.N. West, in: Metallic Alloys: Experimental and Theoretical Perspectives, eds. J.S. Faulkner, R.G. Jordan (Kluwer, Dordrecht, 1994).
[10] B.N. Singh, M. Eldrup, A. Horsewell, P. Ehrhart, F. Dworschak, to be published.
[11] M.J. Puska, R.M. Nieminen, Rev. Mod. Phys. 66 (1994) 841.
[12] P. Asoka-Kumar, K.G. Lynn, D.O. Welch, J. Appl. Phys. 76 (1994) 4935.
[13] K.O. Jensen, R.M. Nieminen, Phys. Rev. B36 (1987) 8219.
[14] T. Korhonen, M.J. Puska, R.M. Nieminen, Phys. Rev. B54 (1996) 15016.
[15] K.O. Jensen, M. Eldrup, B.N. Singh, A. Horsewell, M. Victoria, W.F. Sommer, J. Mater. Sci. Forum 15–18 (1987) 913.
[16] M. Eldrup, B.N. Singh, A. Möslang, J.H. Evans, to be published.

[17] C.H. Woo, B.N. Singh, Philos. Mag. A65 (1992) 889.
[18] M. Eldrup, O.E. Mogensen, J.H. Evans, J. Phys. F6 (1976) 499.
[19] K.O. Jensen, M. Eldrup, B.N. Singh, M. Victoria, J. Phys. F18 (1988) 1069.
[20] B.N. Singh, M. Eldrup, A. Möslang, in: Effects of Radiation on Materials, eds. A.S. Kumar, D.S. Gelles, R.K. Nanstad, E.A. Little, ASTM-STP 1175 (American Society for Testing and Materials, Philadelphia, PA, 1993) p. 1061.